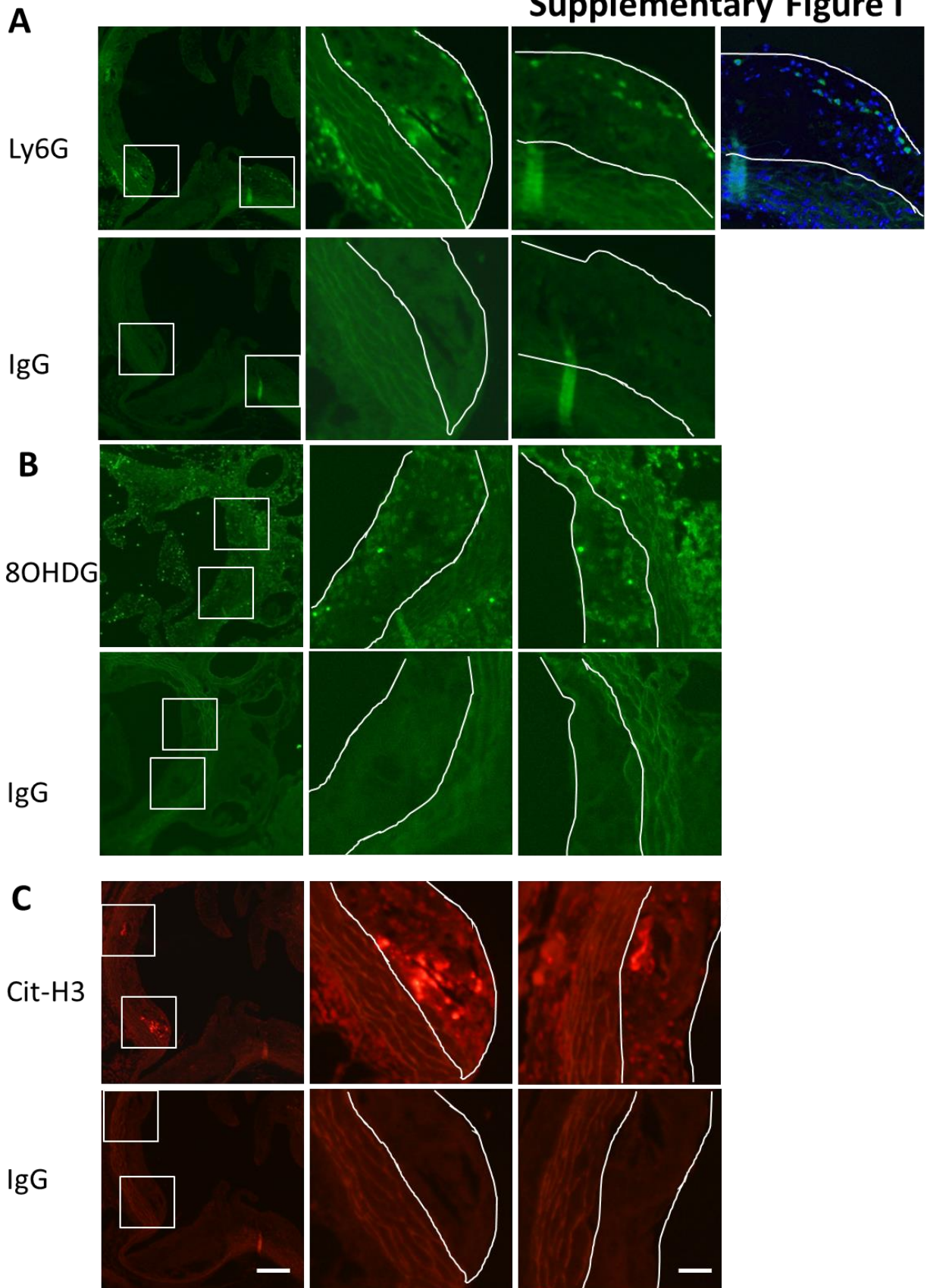


# **Supplementary Figures and Legends**

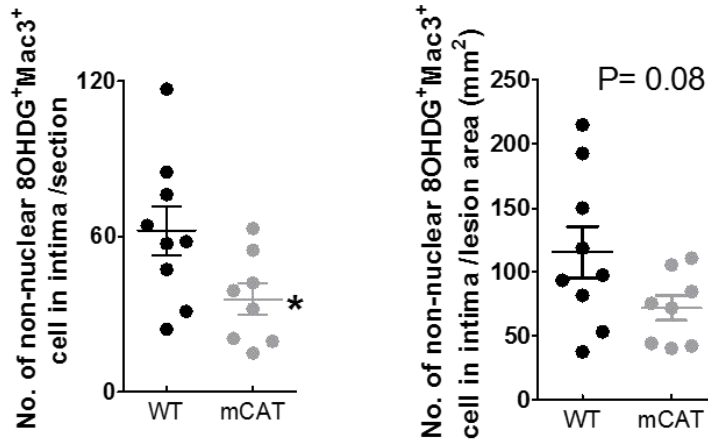
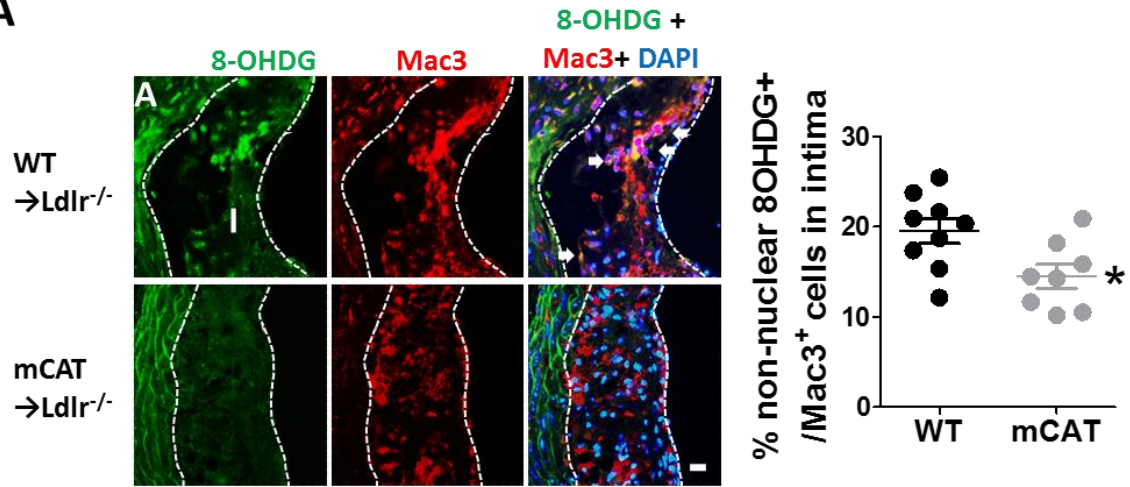
Supplementary Figure I



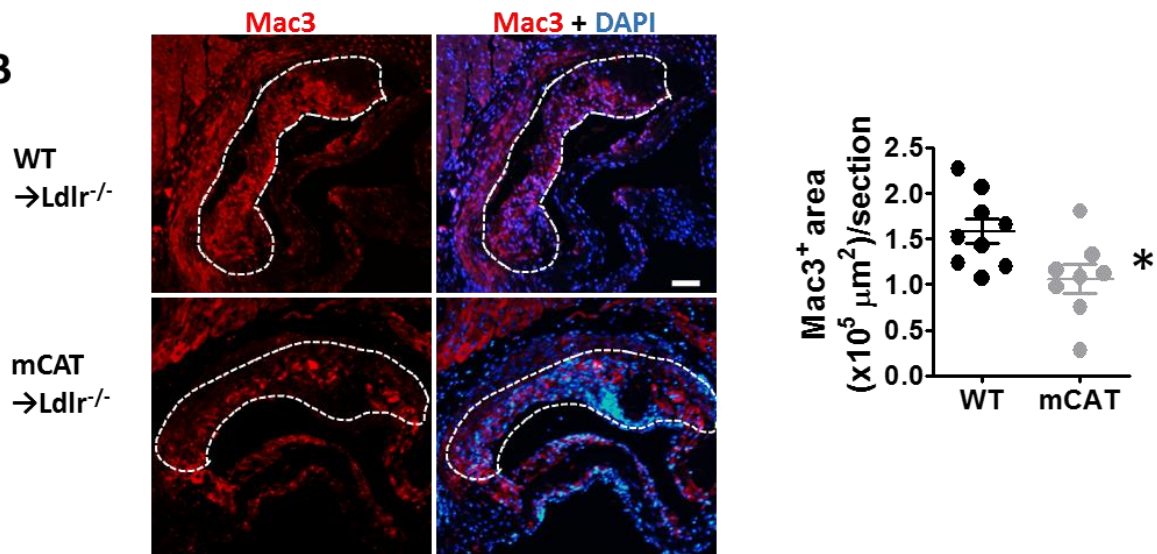
**Supplementary Figure I. Immunostaining of Ly6G, 8OH DG and Citrullinated Histone 3 (Cit-H3) in the atherosclerotic lesions.** Representative images of Ly6G (A), 8OH DG (B) and Cit-H3 (C) vs. their respective isotype control IgG stainings in the aortic root lesions from aged WT→*Ldlr*<sup>-/-</sup> mice. Merged images of Ly6G (green) and counter-stain of nuclei (DAPI, blue) is also shown in (A). The 2<sup>nd</sup> and 3<sup>rd</sup> columns are of higher magnifications of the boxed areas in the 1<sup>st</sup> column. Scale bars, 50 μm (1<sup>st</sup> column) and 15 μm (2<sup>nd</sup> and 3<sup>rd</sup> columns).

## Supplementary Figure II

**A**

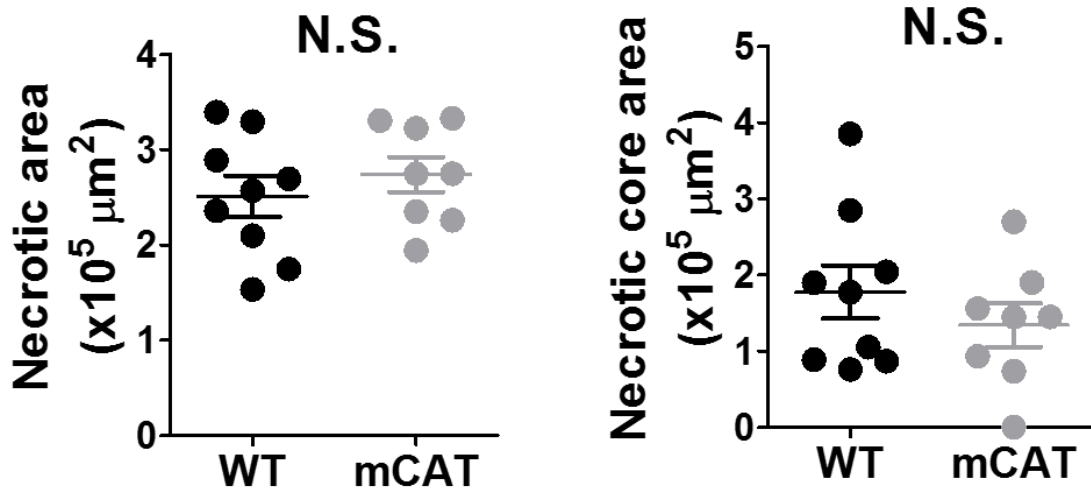


**B**



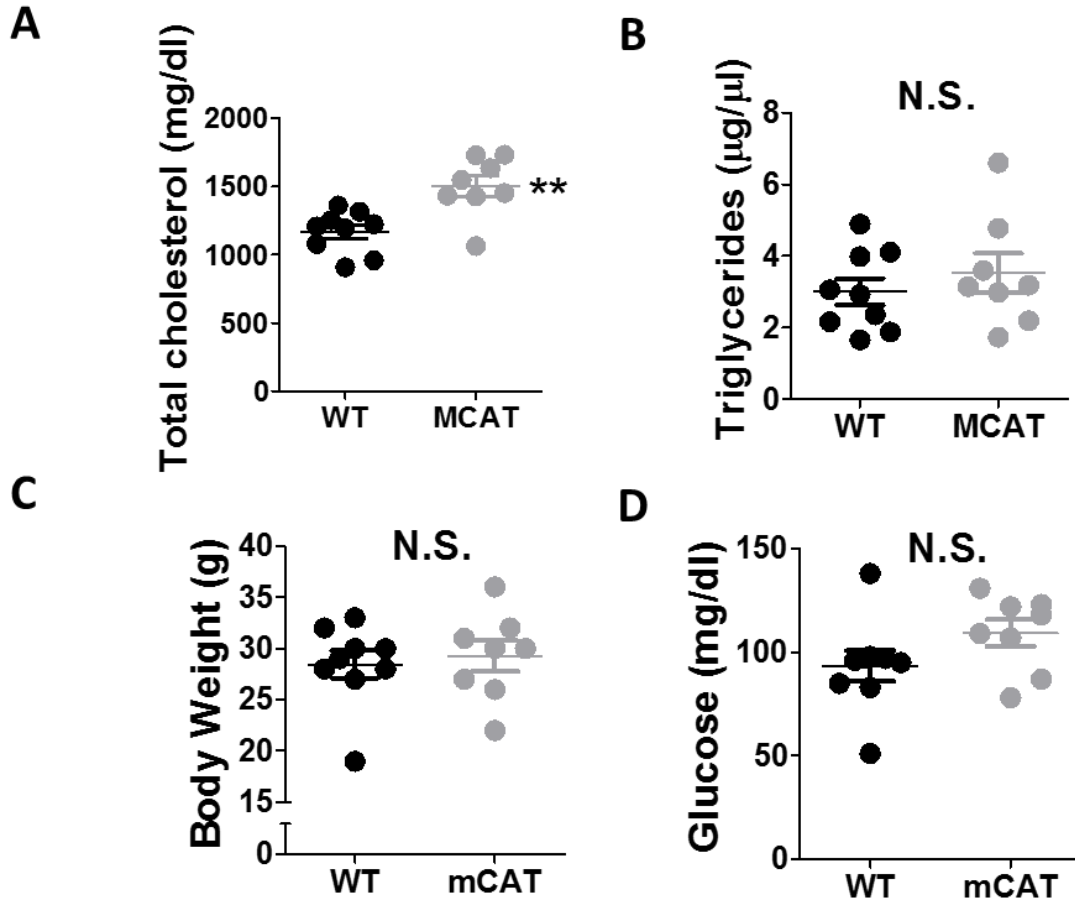
**Supplementary Figure II. Suppression of mitoOS in lesional macrophages and decreased number of macrophages in the atherosclerosis lesions from aged mCAT→Ldlr<sup>-/-</sup> mice.** 36-week-old WT →Ldlr<sup>-/-</sup> and mCAT→Ldlr<sup>-/-</sup> mice were fed the Western-type diet for 16 weeks and aortic root lesions were analyzed. (A) Representative images of non-nuclear 8-OHDG staining (a marker of DNA oxidative damage, green) and Mac3<sup>+</sup> macrophages (red) in the aortic root lesions, with the intima outlined by the dotted line. Images represented 9 WT and 8 mCAT mice. In the merged image, the green 8-OHDG signal co-localizes with the red fluorescence (Mac3) and appears as yellow signals (arrows) in juxtaposed with the blue nuclei. When DNA oxidative damage is suppressed, the green 8-OHDG signal was abrogated and myeloid cells give red signals (arrowheads). Scale bar, 10 μm. A, adventitia; I, intima. Scale bar, 40 μm. Data were quantified as % of non-nuclear 8OHDG<sup>+</sup> among all the Mac3<sup>+</sup> cells in intima, number of non-nuclear 8OHDG<sup>+</sup> Mac3<sup>+</sup> cells in intima per section or number of non-nuclear 8OHDG<sup>+</sup>Mac3<sup>+</sup> cells normalized to lesion area. \*P<0.05 using student's t test. (B) Representative images of macrophage marker Mac3 staining (red) in the lesions from two groups of mice, with the intima outlined by the dotted line. Scale bar, 40 μm. Data were quantified and presented as Mac3<sup>+</sup> area per section. n= 9 WT vs. 8 mCAT; \*P<0.05 using student's t test.

### Supplementary Figure III



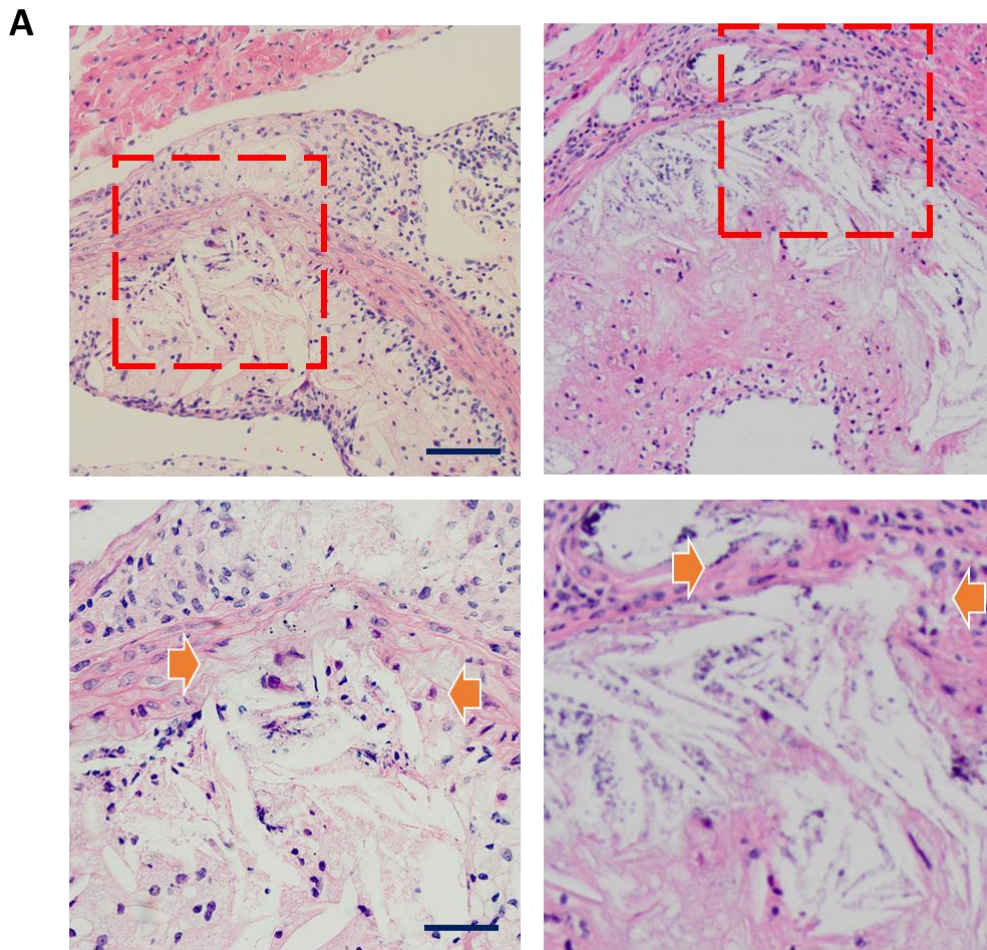
**Supplementary Figure III. Suppression of mitoOS in myeloid cells did not affect necrotic area in the aged mice.** 36-week-old mCAT→*Ldlr*<sup>-/-</sup> and WT →*Ldlr*<sup>-/-</sup> chimeric mice were fed the Western diet for 16 weeks and aortic root lesions were analyzed. Necrotic areas, defined acellular necrotic areas (negative for hematoxylin-positive nuclei) per cross section, were quantified by taking the average of 6 sections spaced 30 μm apart beginning at the base of the aortic root. Using this method, a 97% agreement in the percent necrotic area was calculated between 2 independent observers. Data were quantified as the average necrotic area per section (left plot) and the percentage of necrotic area over total intimal area (right plot). n=9 WT vs 8 mCAT mice; \*P < 0.05 by student's t test; N.S., not significant.

## Supplementary Figure IV



**Supplementary Figure IV. Plasma cholesterol, triglyceride, fasting glucose and body weight of 16wk WD-fed control  $\rightarrow$  *Ldlr*<sup>-/-</sup> and mCAT  $\rightarrow$  *Ldlr*<sup>-/-</sup> mice.** The indicated plasma metabolic parameters were assayed after 12 hour fasting in two groups of mice. n = 9 control vs. 8 mCAT mice; \*\* P < 0.001 using student's t test; N.S., not significant.

## Supplementary Figure V



**B**

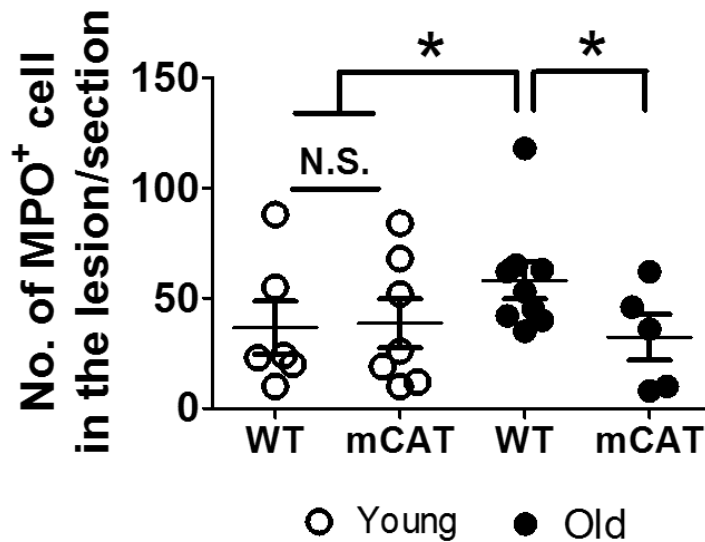
Group	With Erosion	Without Erosion	Total
WT	4	5	9
mCAT	0	8	8

Fisher Exact Probability Test: P = 0.052 (one-tailed)

P = 0.082 (two-tailed)

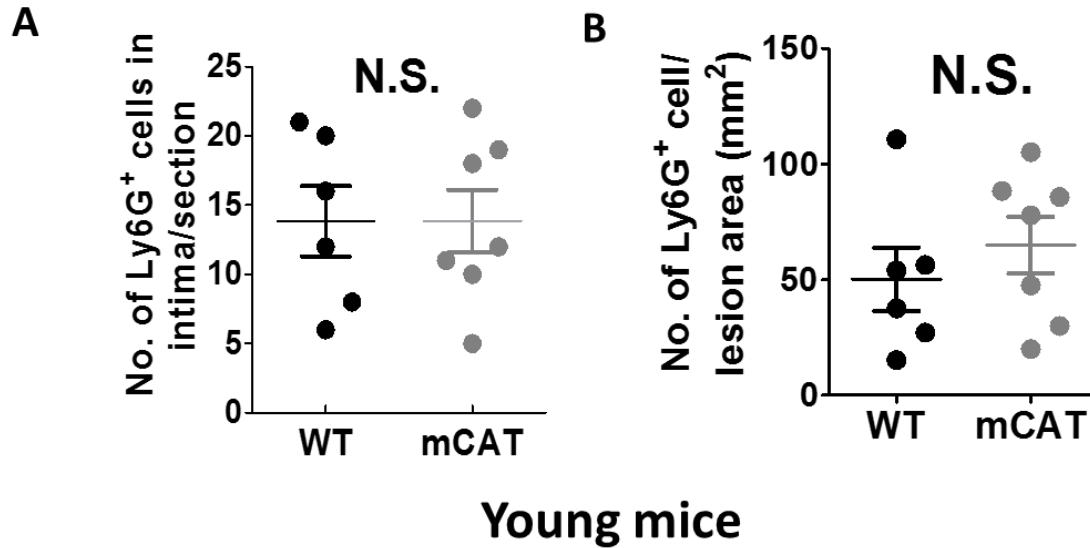
**Supplementary Figure V. Partial degradation of tunica media in aged WT  $\rightarrow$ Ldlr<sup>-/-</sup> chimeric mice.** (A) Shown are examples of hematoxylin and eosin–stained aortic root lesions, with the partial degradation of tunica media depicted by arrows. The lower image is of higher magnifications of the boxed area in the image above. Scale bars, 40  $\mu$ m (upper) and 20  $\mu$ m (lower). (B) The exact number of mice which exhibited partial degradation of tunica media was listed. P = 0.052 (one-tailed) and 0.082 (two-tailed) using Fisher Exact Probability test.

## Supplementary Figure VI



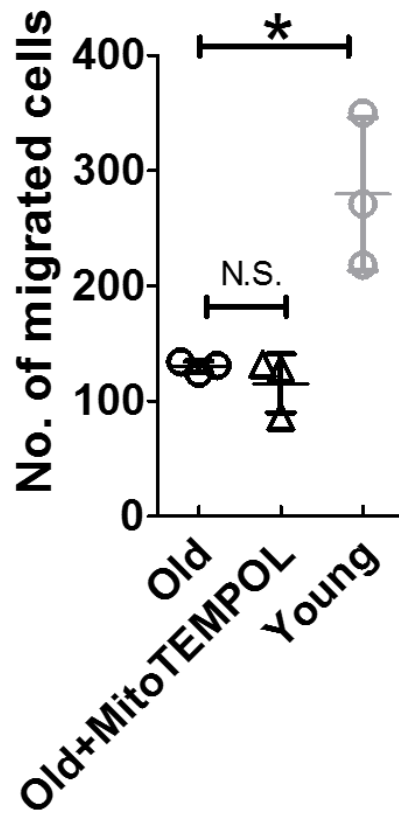
**Supplementary Figure VI. Decreased MPO<sup>+</sup> cells in aged mCAT → Ldlr<sup>-/-</sup> lesions.** 36-week (old) and 14-week (young) old Ldlr<sup>-/-</sup> mice that have been reconstituted with WT and mCAT bone marrows were fed on WD for 16 weeks. Aortic root lesions were stained with antibody against myeloperoxidase (MPO) and counter-stained with nuclei marker DAPI, and analyzed by fluorescent microscope. Data were quantified and presented as No. of MPO<sup>+</sup> cells in intima per section. n = 6 WT vs. 7 mCAT young mice, 9 WT vs. 5 mCAT aged mice. \* P < 0.05 using one-way ANOVA followed by Bonferroni post hoc test. N.S., not significant.

## Supplementary Figure VII



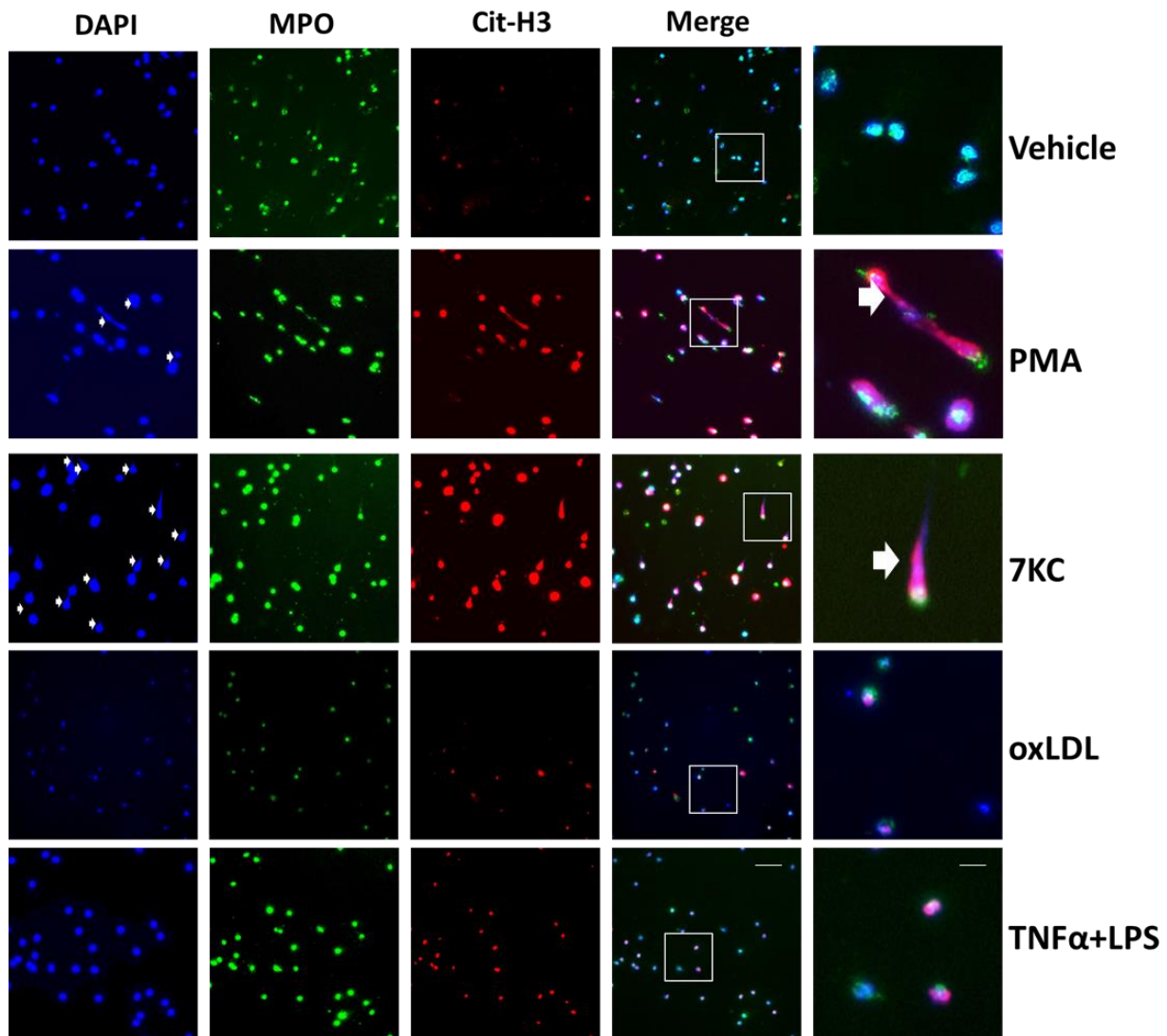
**Supplementary Figure VII. NET formation and Ly6G<sup>+</sup> cells in the lesions from the young mice.** 14-week-old mCAT→*Ldlr*<sup>-/-</sup> and WT →*Ldlr*<sup>-/-</sup> chimeric mice were fed the Western-type diet for 16 weeks and aortic root lesions were analyzed. Aortic root lesions were analyzed using the same procedure as in Figure 1. Data were quantified and presented as No. of Ly6G<sup>+</sup> cell in intima per section and No. of Ly6G<sup>+</sup> cell normalized to lesion area. n= 6 WT vs. 7 mCAT. \*P<0.05 using student's t test.

## Supplementary Figure VIII



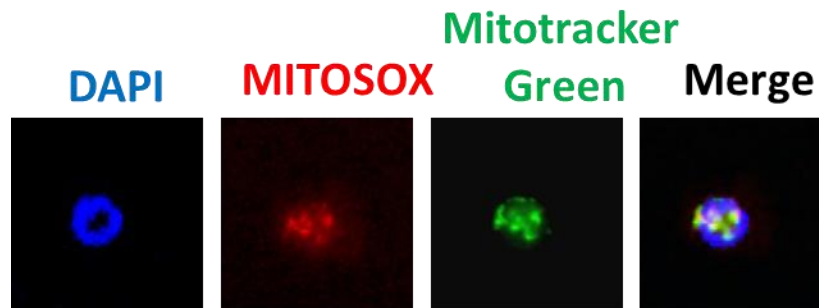
**Supplementary Figure VIII. Neutrophils from aged mice exhibited impaired trans-well migratory capacity toward the formyl chemotactic peptide.** Neutrophil trans-well migration toward formyl chemotactic peptide formyl-Met-Leu-Phe was performed on neutrophils isolated from 3 old (58-week-old) and 3 young (16-week-old) male mice. Cells were allowed to migrate for 2 hrs. In some wells, cells were pretreated with MitoTEMPOL (10 $\mu$ M) for 30 min before being seeded into the insert chamber. 10 $\mu$ M formyl-Met-Leu-Phe was added to the receiver plate. Data were quantified as the number of migrated cells in the receiver plate in each well. Each dot represents the average number of migrated cells in doublet wells from one animal. \*P<0.05 using one-way ANOVA followed by Bonferroni post hoc test. N.S., not significant.

## Supplementary Figure IX



**Supplementary Figure IX. PMA and 7KC, but not oxLDL or LPS primed with TNF- $\alpha$  induced NET in cultured mouse neutrophils.** Neutrophils isolated from 58-week-old C57 WT mice were treated for 4 hr with vehicle, PMA (200 nM), 7KC (50  $\mu$ g/ml), oxLDL (50 $\mu$ g/ml) or LPS (100 ng/ml) with TNF- $\alpha$  priming (10 ng/ml, 15 min). Cells were then fixed with ice-cold acetone, and stained with antibodies against MPO and Cit-H3, counter-stained with DAPI. NETs were depicted by white arrows and were defined as extracellular structures positive for Cit-H3 and DAPI. The 5<sup>th</sup> column is of higher magnifications of the boxed area in the image of 4<sup>th</sup> column. Scale Bars, 40  $\mu$ M (left) and 10  $\mu$ M (right).

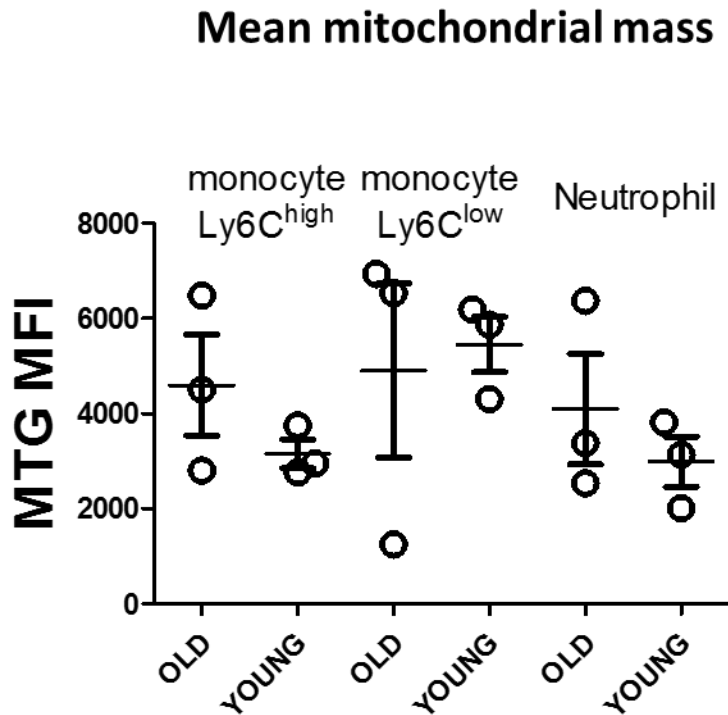
## Supplementary Figure X



### Neutrophil

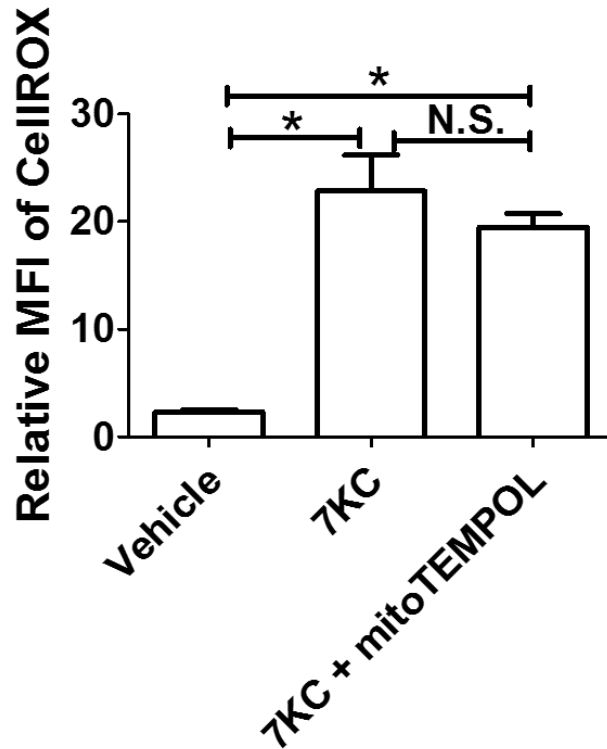
**Supplementary Figure X. Localization of MitoSOX signal with mitochondria in cultured neutrophils.** Neutrophils isolated from WT mice were stained with 5  $\mu$ M MitoSOX (red for mitochondrial superoxide), 100nM Mitotracker Green (MTG, green for mitochondria) and 10ng/ml Hoechst (blue for nuclei) for 15 min at 37°C with 5% CO<sub>2</sub>. Cells were visualized by confocal fluorescence microscopy. Co-localization of MitoSOX with MTG displayed yellow color, which did not overlap with nuclei.

## Supplementary Figure XI



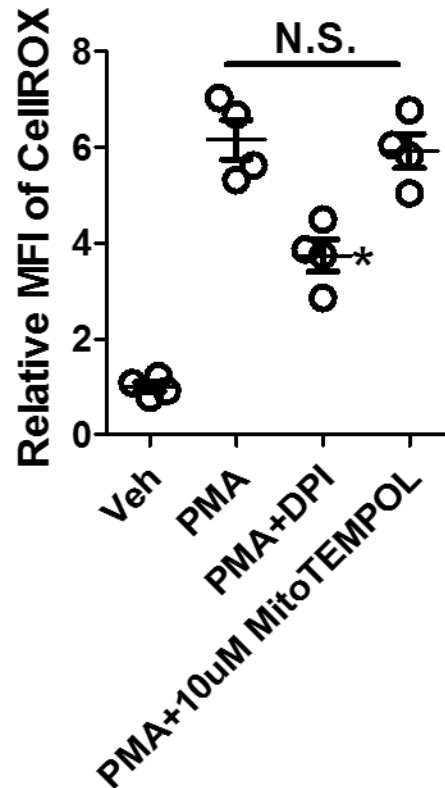
**Supplementary Figure XI. Comparable mitochondrial mass in monocyte and neutrophils from young and old mice.** Peripheral leukocytes from 3 old (58-week) and 3 young (16-week) WT mice were isolated by lysing of RBCs. Leukocytes were further stained with mitotracker green (MTG) and cell surface markers: CD45, CD115 and Gr-1. Using FSC/SSC and CD45<sup>+</sup> gating in FACS analysis, the CD115<sup>+</sup>Gr-1<sup>+</sup> population was defined as Ly6C<sup>high</sup> monocytes; CD115<sup>+</sup>Gr-1<sup>-</sup> population as Ly6C<sup>low</sup> monocytes; and CD115<sup>-</sup>Gr-1<sup>+</sup> as neutrophils. Mitochondrial mass was determined by the mean fluorescent intensity (MFI) of MTG. Each dot represented one animal.

## Supplementary Figure XII



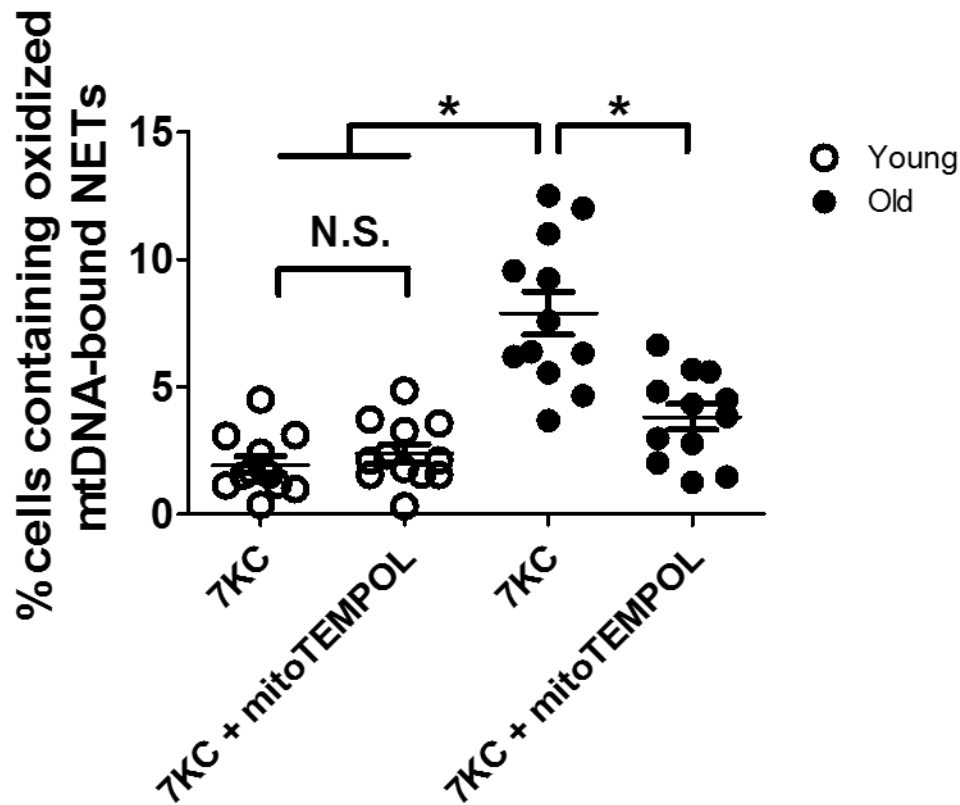
**Supplementary Figure XII. mitoTEMPOL did not decrease cytosolic ROS in neutrophils from aged mice *in vitro*.** Neutrophils isolated from 58-week-old mice were pretreated with vehicle or 10  $\mu$ M mitoTEMPOL for 30 minutes and then incubated with 50 $\mu$ g/ml 7KC for 10 hours. At the end of incubation, cells were stained with 0.6  $\mu$ M cytosolic ROS indicator, CellROX Deep Red (1:4000 dilution) for 20 minutes. The relative cytosolic ROS contents were measured by the MFI of CellROX using flow cytometry. Data represented cells from 2 mice and triplicates for each treatment; \*  $P < 0.05$  using one-way ANOVA followed by Bonferroni post hoc test. N.S., not significant.

## Supplementary Figure XIII



**Supplementary Figure XIII. NADPH oxidase inhibitor DPI, but not mitochondrial ROS inhibitor MitoTEMPOL, suppressed PMA-induced enhancement of cytosolic ROS.** Neutrophils isolated from 4 WT mice were pretreated with vehicle, NADPH oxidase inhibitor DPI (20 $\mu$ M) or mitochondrial ROS inhibitor mitoTEMPOL for 30 min, and then incubated with either vehicle or PMA (200nM) for 3 hr. At the end of incubation, cells were washed with warm medium and stained with 0.6  $\mu$ M cytosolic ROS indicator, CellROX Deep Red (1:4000 dilution) for 20 minutes before flow cytometry analysis. Total cytosolic ROS was quantified as the MFI of CellROX. Each dot represents one animal. \* $P < 0.05$  using one-way ANOVA followed by Bonferroni post hoc test. N.S., not significant.

## Supplementary Figure XIV



**Supplementary Figure XIV. mitoTEMPOL reduced the mtDNA-bound NET formation in neutrophils from aged mice *in vitro*.** Circulating neutrophils purified from 58-week-old (old) and 16-week-old (young) WT mice were pre-incubated with vehicle or 10 $\mu$ M mitoTEMPOL for 30 minutes followed by incubation with 7KC (50 $\mu$ g/ml) for 4 hr. The number of cells which contained NETs bound with material recognized by 8-OHDG antibody (oxidized mtDNA-bound NETs) among all the cells were quantified. \*  $P < 0.05$  using one-way ANOVA followed by Bonferroni post hoc test. N.S., not significant.

## References:

1. Wu J, Li X, Zhu G, Zhang Y, He M, Zhang J. The role of resveratrol-induced mitophagy/autophagy in peritoneal mesothelial cells inflammatory injury via nlrp3 inflammasome activation triggered by mitochondrial ros. *Experimental cell research*. 2016;341:42-53
2. Zhou R, Yazdi AS, Menu P, Tschopp J. A role for mitochondria in nlrp3 inflammasome activation. *Nature*. 2011;469:221-225
3. Hashiguchi N, Chen Y, Rusu C, Hoyt DB, Junger WG. Whole-blood assay to measure oxidative burst and degranulation of neutrophils for monitoring trauma patients. *European Journal of Trauma*. 2005;31:379-388